Short Communication

Thermal Conductivity Models for Polymer Stabilized Hybrid Nanofluids Prepared by One-Step Method

Annie Aureen Albert[1*], D. G. Harris Samuel[2], S. Induja[3] and V. Parthasarathy[1]

[1]Department of Physics, Faculty of Science and Humanities, Hindustan Institute of Technology and Science (Deemed to be University),P.O. Box 1, Padur, Chennai, Tamil Nadu, India
[2]Department of Mechanical Engineering, Faculty of Mechanical Sciences, Hindustan Institute of Technology and Science (Deemed to be University), P. O. Box 1, Padur, Chennai, Tamil Nadu, India
[3]Department of Chemistry, Faculty of Science and Humanities, Hindustan Institute of Technology and Science (Deemed to be University), P. O. Box 1, Padur, Chennai, Tamil Nadu, India

(*) Corresponding author: annieaahits@gmail.com
(Received: 28 January 2022 and Accepted: 09 August 2022)

Abstract

Polyvinyl alcohol (PVA)-ZnO hybrid nanofluid (HNF) was prepared by a one-step chemical method. The structure of PVA-ZnO nanocomposite was concluded by XRD analysis. The stability of HNF was investigated by spectral absorbency analysis and photographic capture methods. 1 wt% PVA capped ZnO nanofluid was stable for 45 days. Zeta potential measurements confirmed that the enhanced stability of PVA-ZnO HNF is due to steric stabilization offered by the polymer. The thermal conductivity of HNFs was predicted by applying the Mixture rule to the conventional Maxwell and Xue models. The theoretical values predicted by the above models were in good agreement with the experimental values. However, it increased steeply with the onset of percolation and it exhibited an additive behaviour under percolation. Thermal conductivity of the prepared hybrid nanofluids increased with temperature and maximum thermal conductivity of the hybrid nanofluids was observed at 60^{o}C with 0.009 weight% of solid dispersant. Theoretical models were used to explain the thermal conductivity of hybrid nanofluids in contrast to most of the reported work which has used empirical correlations. The additive model satisfactorily explained the thermal conductivity of hybrid nanofluids under percolation. TEM micrograph showed the formation of heat conducting path due to onset of percolation in PVA-ZnO HNF resulting 22.5% increase in thermal conductivity due to synergistic effect.

Keywords: *PVA-ZnO nanocomposites, One-step synthesis, Hybrid nanofluids, Thermal conductivity models.*

1. INTRODUCTION

Researchers achieved excellent enhancement in heat transfer efficiency, thermal conductivity and improvement in heat flux by suspending small concentrations of nanoparticles in conventional heat transfer fluids [1]. These fluids are termed as nanofluids and are capable of improving the efficiency; safety and durability of thermal systems. Nanofluids are engineered colloidal suspensions of nanoparticles in a conventional coolant. Nowadays heat transfer problems in the industry are addressed by replacing conventional fluids with nanofluids owing to their promising thermo-physical properties [2].

Nanoparticles such as carbon nanotubes (CNT), carbon nanodots, metals, metallic

oxides, nonmetallic oxides, nonmetallic oxides, carbides and ceramics have been used widely as solid phase dispersants. Various fluids like ethylene glycol, water, mineral oil and poly-olefins are used as dispersing mediums [3].

HNFs are advanced nanofluids that are prepared by suspending two or more dissimilar nanoparticles either in composite or mixture form in the base fluids [4]. Composite nanoparticles possess significant advantages over mono-nanoparticles. HNFs prepared by dispersing nanocomposites exhibit superior performance. Al_2O_3-CuO nanocomposite dispersed in water was used to study the performance of solar absorber unit attached with fin and helical turbulator. The addition of Al_2O_3-CuO nanocomposite raised the Nusselt number (Nu) and Darcy factor (*f*) by 5.26% and 1.52% respectively [5]. The Addition of Al_2O_3-CuO nanocomposite to work fluid increased *Nu, f* and thermal productivity in Fresnel reflector solar systems [6]. Shiekholeslami used hybrid nanofluids in solar systems and reported enhanced heat absorption and improved thermal properties [7].

However, nanofluids lack stability, which leads to degradation of the superior thermo-physical properties. Stability is governed by several factors like particle characteristics, particle concentration, pH of the nanofluid, type of surfactants, viscosity of the base fluid, formulation methods and sonication time [8]. The instability of nanofluids arises from the interaction of nanoparticles with one another during collisions (Brownian motion) leading to aggregation and sedimentation. The stability of nanofluids is still a principal issue that needs to be surmounted as it affects the thermo-physical properties of the nanofluids [9, 10].

The stability of nanofluids is improved by using surfactants to counterbalance the force of attraction between the particles. Two types of stabilization are generally employed namely, steric stabilization and electrostatic stabilization. The pH at which a particular molecule carries no net electrical charge is an isoelectric point. The pH of nanofluids is an important factor for zeta potential. By adjusting the pH to be away from the isoelectric point the nanofluids can be stabilized electrostatically [11, 12].

Polymers are used as surfactants to achieve steric stabilization. The capping of polymers onto the surface of nanoparticles prevents physically the agglomeration of nanoparticles leading to better stability compared to electrostatic stabilization. The concentration of the polymer dispersant directly influences the steric repulsion between the particles [13]. Polymers such as polymethacrylic acid [14], polyvinyl pyrrolidone (PVP) [15], polyvinyl alcohol [16-18] polyethylene glycol [19] are used as steric stabilizers. A combination of PVA and PVP is also used as a stabilizer [20].

Method of preparation influences the stability of nanofluids [9]. Both mono and HNFs are synthesized either by one-step method or two-step methods. However better stability is achieved by the one-step method [13, 21]. One-step physical methods of synthesis employ specialized instruments which are expensive and are not suitable for the bulk production of nanofluids [10].

The one-step chemical method is relatively simple, cost-effective and results in more stable suspensions. The synthesis of HNFs by the one-step chemical method is scarce in the literature. It was observed that most of the research work done using one-step synthesis methods deals only with the synthesis of metallic nanofluids [22].

Practical implementation of nanofluids in heat transfer applications can be achieved by addressing the following: i) the complexity of the preparation process ii) lack of suitable models to compute the thermal conductivity of HNFs [23] and iii) Cost of synthesis [10].

The present investigation aims to overcome the above-mentioned impediments. Hence, in the present

investigation, highly stable PVA-ZnO HNF with enhanced thermal conductivity was prepared by the one-step chemical method. The Mixture rule was incorporated into Maxwell [24] and Xue [25] models to verify the thermal conductivities of two PVA-based HNFs namely: the prepared PVA-ZnO hybrid nanofluid and PVA-CuO hybrid nanofluid reported by Annie et al. (2020a) [18].

ZnO is an antimicrobial, antibacterial, biocompatible and low-cost material [26] with high thermal conductivity [27]. Choudhary et al. (2020) reported that flat plate solar collector efficiency was improved by 19.2% while using ZnO nanofluids [28]. Sheikholeslami incorporated ZnO NPs in paraffin to augment its thermal conductivity and achieved favourable results in the solar thermal storage system [29]. Therefore, ZnO was selected as the dispersant.

PVA is an eco-friendly, non-toxic, non-carcinogenic, versatile biomaterial [30]. It is a water-soluble polymer with a chelating ability. The OH groups present on the surface of metal oxides interact with PVA through a kind of ligand reaction [31, 32]. Tang et al. [14] prepared a nanofluid with long-term stability by dispersing PMMA grafted ZnO nanoparticles in water. Zhang and his colleagues [33] employed PVP and PEG as surfactants to prepare ZnO suspensions by a two-step method. Li et al. [34] synthesized ZnO-ethylene glycol nanofluid with PVP as a stabilizer by a two-step method which was stable for 48 hours. Singh and his colleagues [35] synthesized ZnO-PVA nanofluid by a two-step method to study the dependence of ultrasonic velocity on temperature. Stability of 2 weeks was reported for ZnO nanofluids with PVA as base fluid by Sagadevan et al. [36]. Nagvenkar et al., [37] prepared PVA-ZnO nanocolloid with PVA: Zn acetate ratio of 15:1 and achieved stability for 30 days. The PVA-ZnO HNF prepared by the one-step for this study exhibited better stability for 45 days with a lower PVA: zinc nitrate ratio of 1:3.

This study intends to analyse the influence of the concentration of PVA on the thermal conductivity and stability of PVA-ZnO HNF. Moreover, thermal conductivities of two HNFs namely PVA-ZnO and PVA-CuO are studied using theoretical models, and the estimated theoretical values are compared with the experimental values.

2. EXPERIMENTAL PROCEDURE

2.1. Materials and Methods

All precursors procured for this study were of analytical grade and received from SD Fine Chemicals Ltd., India. The molecular weight of PVA (85% hydrolysed) was 1,25,000. The nanofluids were synthesized by a simple one-step method.1g of polyvinyl alcohol (PVA) was added to 100 ml of deionized water (DI) and stirred rapidly at 60^{o}C for 30 minutes till the complete dissolution of PVA. Then it was mixed with 0.1 M zinc nitrate hexahydrate under stirring conditions. 1.5 M of sodium hydroxide (NaOH) was added gradually to the above solution under constant stirring till the pH of the solution reached 14. The temperature was increased to 80^{o}C and stirring was further continued for 1 hour. A white milky suspension was formed and it was sonicated for 1 hour 15 minutes. Nanofluid preparation was repeated by changing the concentration of PVA in steps of 0.5 g (1.5 g and 2 g).

2.2. Characterization

XRD study was performed using Bruker AXS D8 Advance X-Ray diffractometer with Cu source of wavelength 1.504 A^{o} (CuKα) between10^{o} and 80^{o} (diffraction angles). The particle size was computed using Scherrer's formula:

$$d = 0.9\lambda/(\beta\, cos\theta)$$

Where d – crystallite size, θ - Bragg angle, λ - wavelength of x-ray (CuKα-1.5406 A^{o}) and β - full width at half maximum (FWHM).

The UV-Vis spectra were recorded using the V-670 UV Vis NIR instrument -

JASCO to study the spectral absorption between the wavelengths 200 nm and 800 nm. The size of the particle and morphology of the prepared sample was understood by analysing the recorded HRTEM micrograph using the JEOL/JEM 2100 instrument. . The zeta potential and average hydrodynamic particle size were recorded using a Malvern nano zetasizer (Malvern, UK) with a disposable sizing cuvette cell. The KD2 Pro (Decagon Devices) was used to study the thermal conductivity which operates based on hot-wire method.

2.3. Thermal Conductivity Modelling Strategy

Thermal conductivity models can be arrived at in two ways, either based on (i) hypothesis or (ii) a combination of experimental results and theory. The second method gives a semi-empirical relation [38]. Most of the correlations developed for thermal conductivity ratios of HNFs are empirical [39-42]. These correlations are unique to each nanofluid and new relations need to be developed each time.

However, models based on theoretical modeling can be applied to a wide range of nanofluids. The pioneering work on theoretical modeling of thermal conductivity was done by Maxwell [24]. This model effectively predicts the thermal conductivity ratios of mono nanofluids containing a low volume percentage of spherical NPs.

$$\frac{K_e}{K_b} = \frac{K_p+2K_b-2\phi_p(K_b-K_p)}{K_p+2K_b+\phi_p(K_b-K_p)} \quad (1)$$

where K_e, K_b and K_p are the thermal conductivities of the nanofluid, basefluid and the nanoparticle respectively. However, Maxwell's model could not effectively predict the thermal conductivity of nanofluids containing non-spherical nanoparticles. Hamilton-Crosser model [43], (Eq. 3) considers the increase in surface area of non-spherically shaped particles to conclude the thermal conductivity. This model is given below:

$$\frac{K_e}{K_b} = \frac{K_p+(n-1)K_b-(n-1)(K_b-K_p)\phi_p}{K_p+(n-1)K_b+(K_b-K_p)\phi_p} \quad (2)$$

where ϕ_p - volume fraction and n - shape factor of the nanoparticles.

This model could not predict the thermal conductivity of particles with a large aspect ratio.

Xue [25] proposed a model by considering the spatial distribution of the CNTs based on Maxwell's theory and the large axial ratio. This is given in equation 3.

$$\frac{K_e}{K_b} = \frac{1-\phi_p+\left(\frac{4\phi_p}{\pi}\right)\sqrt{\frac{K_p}{K_b}}\arctan\left(\left(\frac{\pi}{4}\right)\sqrt{\frac{K_p}{K_b}}\right)}{1-\phi_p+\left(\frac{4\phi_p}{\pi}\right)\sqrt{\frac{K_b}{K_p}}\arctan\left(\left(\frac{\pi}{4}\right)\sqrt{\frac{K_p}{K_b}}\right)} \quad (3)$$

Kumar et al. used Xue's model to estimate the thermal conductivity of CNT-based mono NFs [44].

Thermal conductivity models based on hypotheses are rarely explored for HNFs. Takabi and Salehi [45], proposed a hypothesis-based model (equation 4) for HNFs by applying the mixture rule in the Maxwell model. Subramanian and Ilangovan used Maxwell model to calculate the thermal conductivity of Cu_2O-TiO_2 composite nanofluids applying mixture rule but the morphology of the nanocomposite is not discussed [46]

$$\frac{K_{hf}}{K_{bf}} = \frac{\frac{(\phi_{p1}K_{p1}+\phi_{p2}K_{p2})}{\phi_p}+2K_b+2(\phi_{p1}K_{p1}+\phi_{p2}K_{p2})-2\phi K_b}{\frac{(\phi_{p1}K_{p1}+\phi_{p2}K_{p2})}{\phi_p}+2K_b-(\phi_{p1}K_{p1}+\phi_{p2}K_{p2})+\phi K_b} \quad (4)$$

Sheikholeslami et al. used the theoretical model for calculating the thermal conductivity ratio of MWCNT-Al_2O_3 HNF, however, there is no mention of the following factors namely the spatial distribution of MWCNTs and their axial ratio [47].

In this research work, we adopt the following strategy to explain the thermal conductivity ratios (K_e/K_b) of HNFs by considering the morphology of the nanocomposites. The strategy adopted to

compute the thermal conductivity of HNFs is illustrated in Figure 1.

Thermal conductivity of the PVA-ZnO and PVA-CuO HNFs are also evaluated using two methods. In the first method, thermal conductivities of the two HNFs namely PVA-ZnO and PVA-CuO were evaluated by applying the mixture rule (equations (5) and (6)) to the Maxwell model [24] in equation (1) and as well as Xue model [25] in equation (3). The total volume fraction of particles in the HNF is:

$$\phi_p = \phi_{p1} + \phi_{p2} \quad (5)$$

and thermal conductivity of PVA-metal oxide nanocomposite is:

$$K_p = (\phi_1 K_{p1} + \phi_2 K_{p2})/(\phi_p) \quad (6)$$

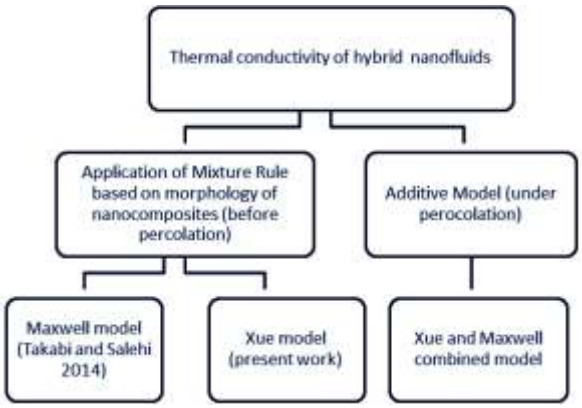

Figure 1. *Schematic representation of the strategy used to explain the thermal conductivity of hybrid nanofluids.*

The second method is an additive model and is used to elucidate the anomalous enhancement in thermal conductivity of PVA-CuO under percolation. The additive model is proposed by adding the thermal conductivity ratios of PVA with basefluid (predicted by Xue's model) and the thermal conductivity ratios of metal oxide nanoparticles with basefluid (predicted by Maxwell's model). The additive model is given in Eq. 7;

$$\frac{K_e}{K_b} = \frac{1-\phi_{p1}+\left(\frac{4\phi_{p1}}{\pi}\right)\sqrt{\frac{K_{p1}}{K_b}}\arctan\left(\left(\frac{\pi}{4}\right)\sqrt{\frac{K_{p1}}{K_b}}\right)}{2\left(1-\phi_{p1}+\left(\frac{4\phi_{p1}}{\pi}\right)\sqrt{\frac{K_b}{K_{p1}}}\arctan\left(\left(\frac{\pi}{4}\right)\sqrt{\frac{K_{p1}}{K_b}}\right)\right)} + \frac{K_{p2}+2K_b-2\phi_{p2}(K_b-K_{p2})}{2(K_{p2}+2K_b+\phi_{p2}(K_b-K_{p2}))} \quad (7)$$

The thermal conductivity of the PVA-ZnO HNF was estimated by hot-wire method. The hot wire is a vertical linear heat source, and the measurement of thermal conductivity is based on Fourier's law. The data is reported as a ratio of thermal conductivity of NF to that of the base fluid. KS-1 Probe (1.3mmX6cm) was used for measuring the thermal conductivity of nanofluid. The accuracy of the device was ±5% (within the measuring range). The device was calibrated with glycine and 97.5% accuracy was recorded. The measurements were repeated 5 times and averaged. The standard deviation was 2.1%. The measured values were compared against theoretical values. The thermal conductivity of PVA, nano ZnO and nano CuO was considered as 0.31W/m/K, 29 W/m/K and 69 W/m/K [48] respectively.

3. RESULTS AND DISCUSSION

3.1. Structural Analysis

Figure 2 depicts the XRD pattern of the ZnO nanoparticles. The assigned diffraction peaks at 2θ of 31.6° (100), 34.2° (002), 36.1° (101), 47.3° (102), 56.3° (110), 62.5° (103), 67.7° (112) and 68.9° (201) are associated with wurtzite (JCPDS 36-1451) structure of ZnO nanoparticles (JCPDS 36-1451) [49].

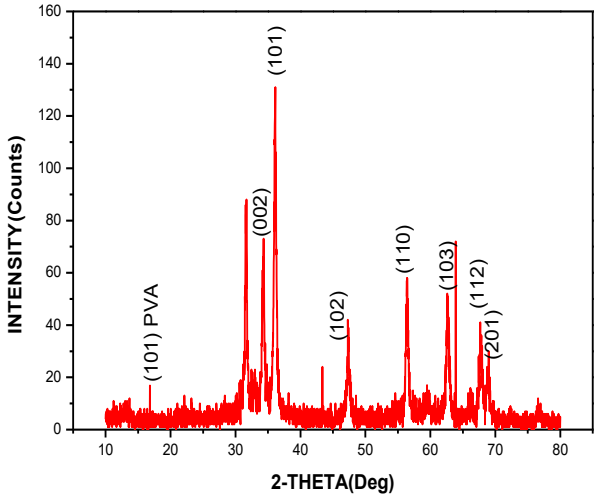

Figure 2. *XRD pattern of ZnO nanoparticles.*

The average grain size was estimated to be 22.94 nm. The shift in the characteristic diffraction peak (101) of PVA indicated

the formation of PVA-ZnO nanocomposite [50].

3.2. Spectral Absorbency

The UV absorption intensity of a suitably diluted nanofluid is directly proportional to the concentration of the nanoparticles suspended in the base fluid [51]. Therefore, the spectral absorbency values are used to study dispersion stability [52]. The stability of PVA-ZnO HNF was evaluated by studying its UV-Vis absorption spectra (Figure 3). The nanofluids exhibited a peak near 346 nm which confirmed the formation of PVA-ZnO nanocomposite [53].The peaks were blue-shifted in comparison to the bulk ZnO observed at 375 nm [37]. This confirmed the nanosize of ZnO. The absorption intensity of PVA-ZnO HNF increased with the increasing concentration of PVA. This was expected and can be explained as follows.

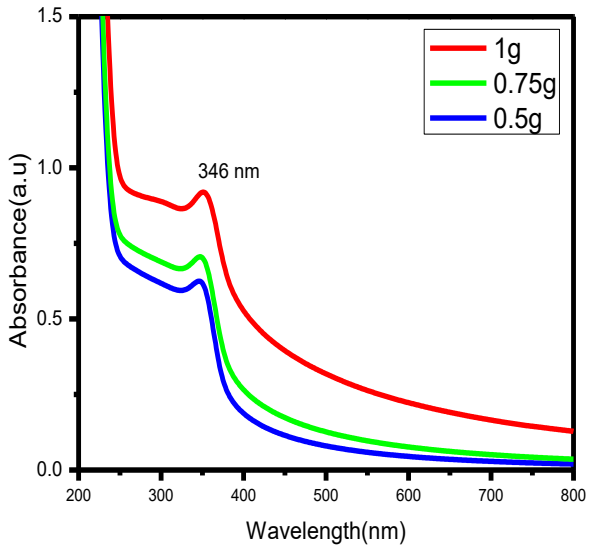

Figure 3. *UV spectrogarph of PVA capped ZnO nanoparticles*

The increase in the concentration of PVA increased steric hindrance (arising from the hydrophilic nature of PVA) between the ZnO nanoparticles preventing the agglomeration of ZnO nanoparticles and subsequent settling down of the particles. Thus there was an enhancement in the stability of the nanofluids while increasing the concentration of PVA.

3.3. Dispersion Stability Using Photographs

Dispersion stability can also be established qualitatively by comparing the photographs of the nanofluids captured at different time intervals [52]. Stability is indicated by absence of visual sedimentation [54]. Figure 4a shows the photograph of the nanofluids captured immediately after synthesis, while Figure 4b shows photographs after 40 days of synthesis. It showed that the PVA-ZnO hybrid nanofluids were stable for more than 40 days which confirmed the enhanced stability of PVA-ZnO HNF as compared with the earlier reports [36, 37, 53].

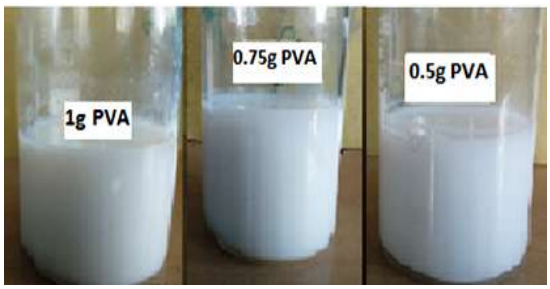

Figure 4. (a) *Photograph of the nanofluids immediately after synthesis*

Figure 4. (b) *Photographs after 40 days of synthesis*

3.4. Morphology Analysis

Figures5a&5b illustrate the HRTEM micrographs of PVA-ZnO HNF with 1 wt% and 0.5 wt% of PVA. Agglomeration of ZnO nanoparticles took place for the PVA-ZnO hybrid nanofluid containing 0.5 wt% of PVA due to inadequate steric hindrance at a low concentration of PVA. The increase in steric hindrance while increasing the concentration of PVA results in a smaller size of the ZnO nanoparticles with lesser agglomeration (Figure 5a). Figure 5c & d shows that the

aggregates are composed of hexagon-shaped crystallites. The insets in Figure 5c & d shows the SAED patterns of PVA-ZnO nanocomposites. It is observed that the samples are polycrystalline and the increase in PVA concentration led to a decrease in the crystalline nature of the nanocomposite.

3.5.Particle Size Analysis

The hydrodynamic particle size obtained by the DLS method was found to be much higher than the size of the PVA-ZnO nanocomposite measured by TEM [55].

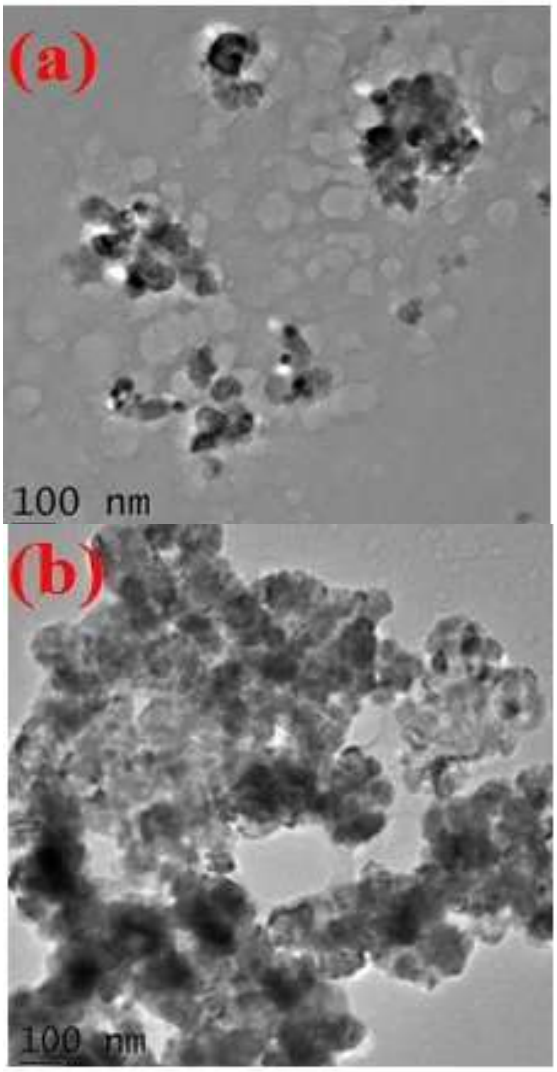

Figure 5. (a) *HRTEM micrograph of 1 wt% PVA-ZnO HNF at 100 nm resolution* ***(b)*** *0.5 wt% PVA-ZnO HNF at 100 nm resolution*

The hydrodynamic size of the particle obtained from DLS is a measure of the size of the nanocomposite, which includes the nanoparticle, the polymer coating and the thickness of the solvent layer that moves along with the particle. The hydrophilic nature of the PVA matrix leads to the formation of a solvent layer around the nanocomposite. This results in a larger value of particle size when measured by the DLS method. The variation of particle size with different concentrations of the dispersant is depicted in Figure 6a-c. It is observed that the hydrodynamic size decreases from 313 nm to 255 nm with an increase in the concentration of PVA from 0.5 wt% to 1 wt% (Table 1).

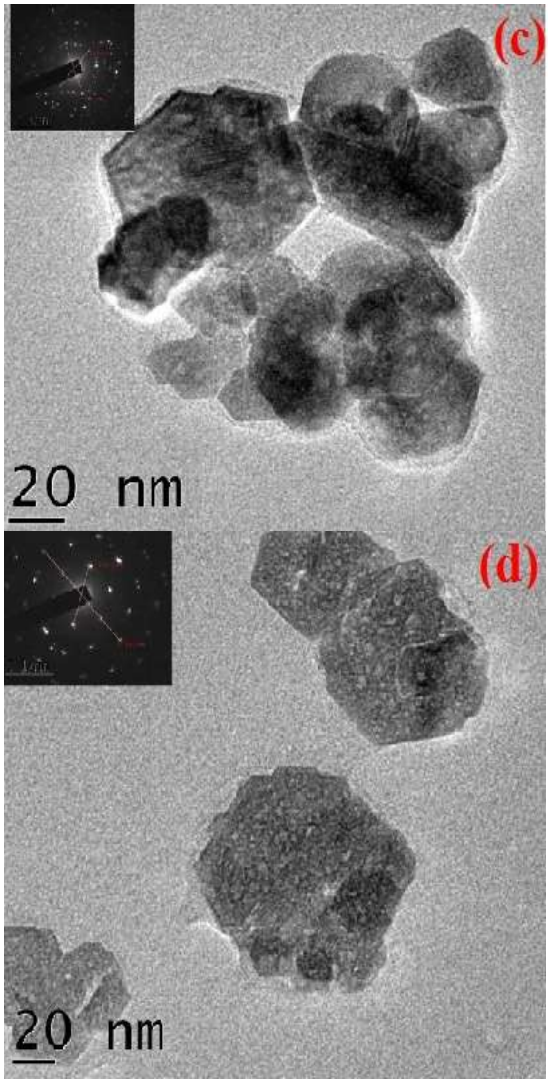

Figure 5. (c) *HRTEM micrograph of 1 wt% PVA-ZnO HNF at 20 nm resolution* ***(d)*** *0.5 wt% PVA-ZnO HNF at 20 nm resolution*

This is due to the improvement in steric hindrance with the increasing PVA concentration.

3.6. Zeta Potential

Zeta potential analysis was performed to comprehend the stability of PVA-ZnO HNFs. Zeta potential is the potential difference between the stern layer which is linked to the particle (dispersed phase) and the bulk liquid or the dispersion media. Measurement of zeta potential is based on estimating the velocity of nanoparticles moving under applied potential through Doppler anemometry.

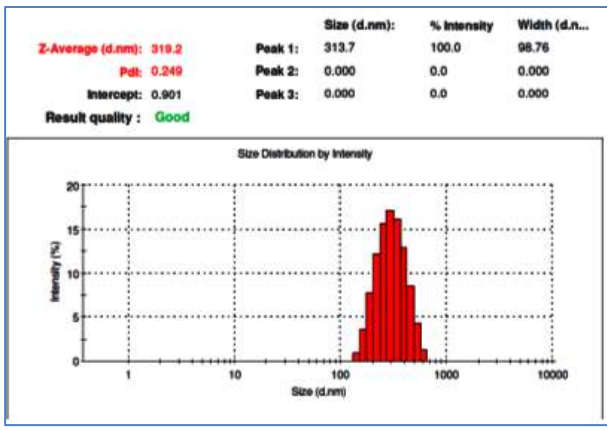

Figure 6. (a) *Particle size distribution of 0.5wt% PVA capped ZnO by DLS.*

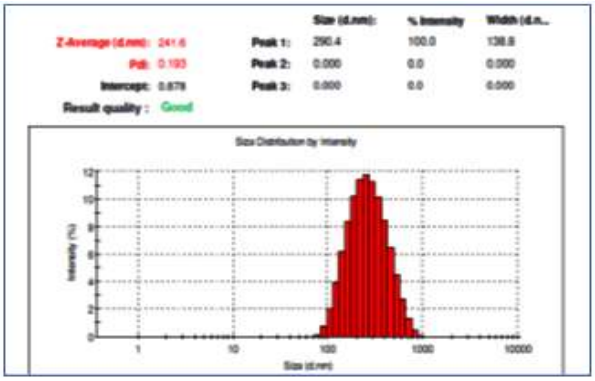

Figure 6. (b) *Particle size distribution of 0.75 wt% PVA capped ZnO by DLS.*

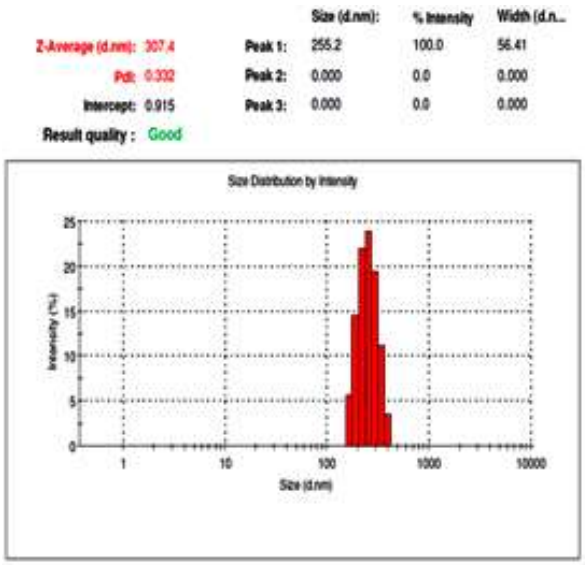

Figure 6. (c) *Particle size distribution of 1wt% PVA capped ZnO by DLS.*

Zeta potential values lying between +30 mV to -30 mV are generally known to exhibit lower stability whereas nanofluids with absolute values greater than 30 mV are considered stable [38].

Table1. *Variation of hydrodynamic size of PVA-ZnO nanocomposite with concentration of PVA*

Concentration of PVA in wt%	Particle size from (high intensity peak) in nm
0. 5	313
0.75	290
1	255

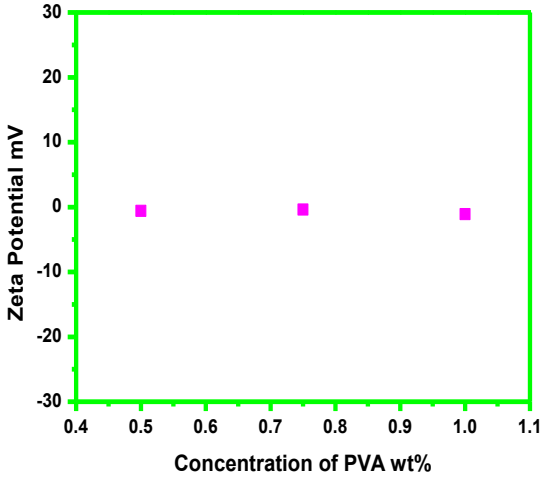

Figure7. *Zeta potential values for varying concentrations of PVA*

Figure7a-c shows the zeta potential measurements for the prepared PVA-ZnO HNFs by varying the concentrations of PVA. The measured zeta potential values are less than -2 mV. However, the HNF is highly stable under visual observation. The improved stability exhibited by the HNF at low values of zeta potential suggests steric stabilization. This observation is similar to the observation of Almeida et al. [56] Steric stabilization of HNF is expected due to the formation of PVA-ZnO nanocomposite [57].

3.7. Thermal Conductivity of Hybrid Nanofluids

The thermal conductivity ratios (K_e/K_b) of PVA-ZnO HNFs for three different concentrations at different temperatures [58] are shown in Table 2.

Table 2. *Thermal conductivity ratios of ZnO-PVA hybrid nanofluid measured at different temperatures for various concentrations of PVA.*

Temperature in (^{O}C)	K_e/K_b values for various concentrations of PVA		
	1 g	0.75g	0.5g
30°C	1.08	1.00	0.99
40°C	1.27	1.24	1.22
50°C	1.39	1.32	1.28
60°C	1.41	1.34	1.33

It is evident from the plots (Figure 8a) that the thermal conductivity ratios of the HNFs increase with temperature for all the concentrations of PVA. This is in agreement with the observations of Kanti et al. [59].

Thermal conductivity ratios of the PVA-ZnO HNFs are evaluated by (i) applying the mixture rule to Maxwell's model [34] (ii) applying the mixture rule to the Xue model [18] and (iii) by summing the thermal conductivity ratios obtained by the Xue model for PVA and Maxwell model for ZnO. Thermal conductivity ratios of PVA-ZnO HNFs predicted by the models mentioned above are compared with the measured values by the hot wire method as shown in Figure 8b.

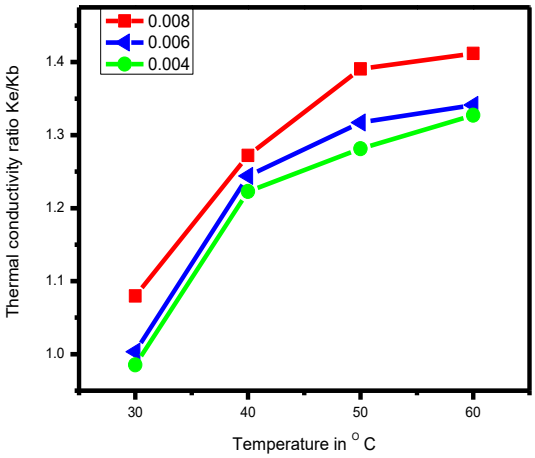

Figure 8. (a) *Variation of thermal conductivity ratio with temperature and volume fraction of PVA*

The values are listed in Table 3.

Table 3. *Thermal conductivity ratios of ZnO-PVA hybrid nanofluid obtained from models and measurement.*

Vol. fraction of solid dispersants in HNF	**Ratio of K_e/K_b for PVA-ZnO HNFs**			
	Maxwell Mixture Rule	**Xue Mixture Rule**	**Maxwell –Xue Models combined Summation Model**	**Experimental values**
0.009	1.019	1.027	2.002	1.08
0.007	1.016	1.024	2.003	1.00
0.005	1.013	1.021	2.003	0.99

The obtained thermal conductivity ratios (K_e/K_b) for different volume fractions of solid dispersant match closely with values obtained by applying the mixture rule in the Maxwell model at low PVA concentrations, due to hexagonal-shaped nanoparticles. However, the thermal conductivity ratio increases sharply at 0.009 volume% of PVA-ZnO nano-composite. This increase is due to the onset of percolation at higher volume concentrations. The long-chain PVA

molecules form a continuous network at s higher concentration which provides a path for the conduction of heat as illustrated in Figure 8c.

The thermal conductivity ratio of K_e/K_b for PVA-CuO HNF containing 0.5 wt% PVA predicted by applying the mixture rule to the Xue model is closer to the measured values (Table 4). It is evident from the graph (Figure 8d) that the observed thermal conductivity ratios of PVA-CuO HNF at low concentrations of PVA are close to the values predicted by applying the mixture rule to the Xue model. This is due to the nanoribbon morphology of PVA-CuO nanocomposite which possesses a high aspect ratio. There is a steep increase in the measured value of thermal conductivity ratios as compared with the predicted values at 0.75g of PVA.

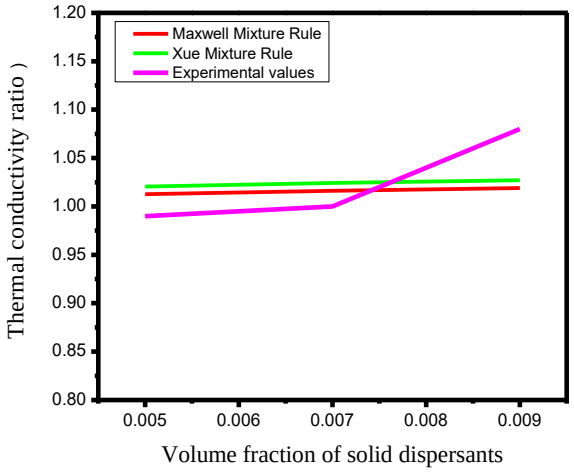

Figure 8. (b) *Thermal conductivity ratio variation for PVA-ZnO HNF with concentration of PVA*

Table 4. *Thermal conductivity ratios of CuO-PVA hybrid nanofluid*

Conc. of PVA-CuO HNF (in vol%)	Vol. fraction of solid dispersants in HNF	Ratio of K_e/K_b for PVA-CuO			
		Maxwell Mixture Rule	Xue Mixture Rule	Maxwell –Xue Models combined Summation Model	Experimental values
100	0.009	1.022	1.039	1.993	1.80
75	0.007	1.017	1.029	1.995	1.70
50	0.004	1.011	**1.019**	1.997	**1.18**
100	0.009	1.022	1.039	**1.993**	**1.80**

This increase is attributed to the formation of percolating structures. As the concentration of PVA increases, the thermal conductivity ratios of PVA-CuO hybrid nanofluids match closely with the additive model indicating a synergistic effect between PVA and CuO nanoparticles at higher concentration

4. CONCLUSION

The structure of PVA-ZnO nanocomposite was confirmed by spectroscopic analysis.

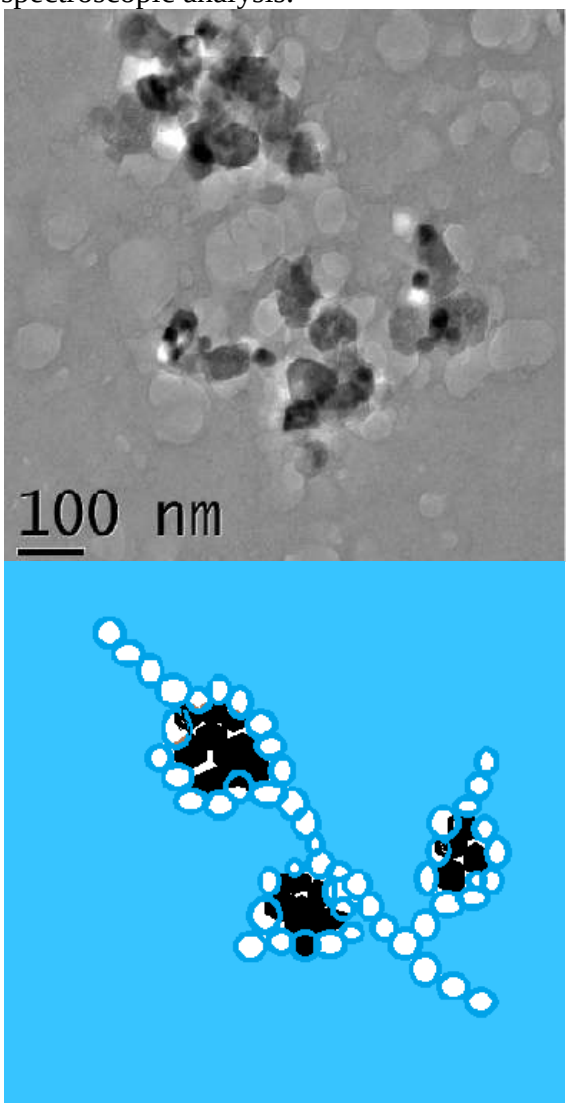

Figure 8. (c) *Heat conducting path due to percolation in PVA-ZnO HNF resulting in synergistic effect.*

The thermal conductivity and stability of HNFs increased while increasing the concentration of PVA. Stability was found to be highest for 1wt% of PVA and maximum enhancement of thermal conductivity (k_{eff} reaching 1.412) was also observed at 60 ^{o}C for the same sample. The size of the PVA-ZnO nanocomposite was computed as 60 – 70 nm by HRTEM. It was concluded that PVA-ZnO was stabilized sterically due to the observed low zeta potential value (-2 mV).The enhanced stability of 40 days can be attributed to the in-situ synthesis of nanofluid and steric stabilization offered by PVA.

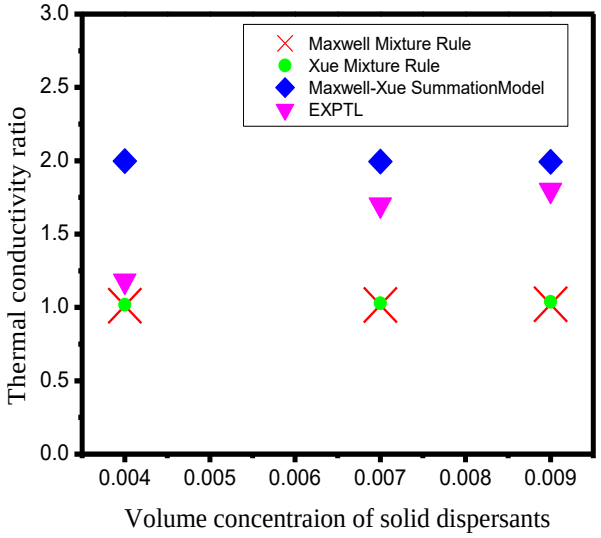

Figure 8. (d) *Thermal conductivity variation of PVA-CuO hybrid nanofluid with concentration of PVA*

The thermal conductivity ratios of PVA-ZnO HNFs matched closely with the Mixture rule applied to the Maxwell model at a low concentration of PVA. The thermal conductivity ratios of PVA-CuO HNFs match closely with the values predicted by applying the mixture rule to the Xue model at a low concentration of PVA. This study suggests that the model employed for predicting the thermal conductivity ratios of HNFs is governed by the morphology of the dispersed nanocomposite. Moreover, in-situ capped PVA-ZnO nanofluid can be considered a suitable candidate for heat transfer applications due to its enhanced stability and thermal conductivity. TEM showed an establishment of heat conducting path due to onset of percolation in PVA-ZnO HNF resulting in a synergistic effect resulting 22.5% increase in thermal conductivity.

Future studies can be done by verifying the thermal conductivity of other HNFs containing long aspect ratio nanoparticles in them by incorporating the mixture rule in Xue's model.

ACKNOWLEDGEMENT

The authors gratefully acknowledge the support of Dr. P. Raghavan, Professor, Department of Chemistry, Hindustan Institute of Technology and Science by providing sonication facilities.

CONFLICT OF INTEREST

Authors declare that there is no potential conflict of interest.

REFERENCES

1. Said, Z., Sharma, P., Tiwari, A. K., Le, V. V., Huang, Z., V. G. Bui, Hoang, A. T., " Application of novel framework based on ensemble boosted regression trees and Gaussian process regression in modelling thermal performance of small-scale Organic Rankine Cycle (ORC) using hybrid nanofluids*", Journal of Cleaner Production*, 360 (2022) 132194.
2. Sharma, P., Said, Z., Kumar, A., Nižetić, S., Pandey, A., Hoang, A. T., Huang, Z., Afzal, A., Li, C., Le, A. T., Nguyen, X. P., Tran, V. D., " Recent Advances in Machine Learning Research for Nanofluid-Based Heat Transfer in Renewable Energy System", *Energy Fuels*; 36 (2022) 6626-6658.
3. Dolatabadi, N., Rahmani, R., Rahnejat, H., Garner, C. P., "Thermal conductivity and molecular heat transport of nanofluids", *RSC Advances*; 9 (2019) 2516.
4. Nabil, M. F., Azmi, W. H., Hamida, K.A., Zawawi, N. N. M., Priyandoko, G., Mamat, R., "Thermo-physical properties of hybrid nanofluids and hybrid nanolubricants: A comprehensive review on performance", *International Communications in Heat and Mass Transfer*, 83 (2017) 30-39.

5. Sheikholeslami, M. , Farshad, S. A., "Nanoparticles transportation with turbulent regime through a solar collector with helical tapes", *Advanced Powder Technology*, 33 (2022) 103510
6. Sheikholeslami, M.., "Numerical investigation of solar system equipped with innovative turbulator and hybrid nanofluids", *Solar Energy Materials and Solar Cells*, 243 (2022) 111786
7. Sheikholeslami, M.., Ebrahimpour, Z., "Nanofluid performance in a solar LFR system involving turbulator applying numerical simulation", *Advanced Powder Technology*, 33 (2022) 103669.
8. Yang, L., Ji, W., Mao, M., Huang, J-N., "An updated review on the properties, fabrication and application of hybrid-nanofluids along with their environmental effects", *Journal of Cleaner Production*, 257 (2017) 120408.
9. Verma, R., Gupta, K. K., "An insight of synthesis, stability and thermophysical properties of hybrid nanofluids", *IOP Conference Series: Materials Science,* (2020) *810, 2nd International Conference on Emerging trends in Manufacturing, Engines and Modelling (ICEMEM -2019) 23-24 December 2019, Mumbai, India.*
10. Xiong, Q., Altnji, S., Tayebi, T., Izadi, M., Hajjar, A., Sundén, B. Li, L. K. B.,"A comprehensive review on the application of hybrid nanofluids in solar energy collectors", *Sustainable Energy Technologies Assessments*, 47 (2021) 101341
11. Encapsulation of Active Molecules and Their Delivery System Edited by: Sonawane, S. H., Bhanvase, B. A., Sivakumar, M., in "Nanofluids-based delivery system, encapsulation of nanoparticles for stability to make stable nanofluids*",* Thakur, P. Bhanvase, B. A, (2020).
12. Yu, F., Chen, Y., Liang, X., Xu, J., Lee, C., Liang, Q., Tao, P., Deng, T., "Dispersion stability of thermal nanofluids", *Progress in Natural Science,* 27 (2017) 531-542.
13. Yu, W., Xie, H., "A review on nanofluids: preparation, stability mechanisms, and applications", *Journal of Nanomaterials*, 435873 (2012) 1–17.
14. Tang, E., Cheng, G., Ma, X., Pang, X., Zhao, Q., "Surface modification of zinc oxide nanoparticle by PMAA and its dispersion in aqueous system", *Applied Surface Science,* 252 (2006) 5227–5232.
15. Sahooli, M., Sabbaghi, S., Shariaty, N. M., "Preparation of CuO/Water Nanofluids Using Polyvinylpyrolidone and a Survey on Its Stability and Thermal Conductivity". *International Journal of Nanoscience and Nanotechnology*, 8 (2012) 27-34.
16. Jung-Yeul, J**.,** Eung, S. K., Yong, T. K., "Stabilizer effect on CHF and boiling heat transfer coefficient of alumina/water nanofluids*", International Journal of Heat and Mass Transfer*, 55 (2012) 1941-1946. DOI:10.1016/j.ijheatmasstransfer.2011.11.049
17. Annie, A. A., Harris, D. G. S., Parthasarathy, V., Kiruthiga, K., "A facile one pot synthesis of highly stable PVA–CuO hybrid nanofluid for heat transfer application", *Chemical Engineering Communications*, 207 (2020a) 319-330.
18. Annie, A. A., Harris, D. G. S., Parthasarathy, V., "Wet Chemical Synthesis of CuO-PVA Hybrid Nanofluid Stabilized by Steric Repulsion", *Asian Journal of Chemistry*, 32 (2020b) 570-574.
19. Maji, N. C., Krishna, H. P., Chakraborty, J., "Low-cost and high-throughput synthesis of copper nanopowder for nanofluid applications", *Chemical Engineering Journal*, 353 (2018) 34-45.
20. Pavithra, K. S., Gurumurthy, C., Yashoda, M. P., Mateti, T., Ramam, K., Nayak, R., Murari, M. S., "Polymer‐dispersant‐stabilized Ag nanofluids for heat transfer Applications", *Journal of Thermal Analysis and Calorimetry*, 146 (2021) 601–610.
21. Kumar, D. D. and Arasu, A. V., "A comprehensive review of preparation, characterization, properties and stability of hybrid nanofluids", *Renewable and Sustainable Energy Reviews*, 81 (2018) 1669-1689.
22. Shenoy, U. S., Shetty, A. N., "Simple glucose reduction route for one-step synthesis of copper nanofluids", *Applied Nanoscience*, 4 (2014) 47–54.
23. Babar, H., Ali, H. M., "Towards hybrid nanofluids: Preparation, thermophysical properties, applications, and challenges", *Journal of Molecular Liquids*, 281 (2019) 598–633.
24. Maxwell, J. C. "*A Treatise on Electricity and Magnetism*", vol. 1, Clarendon Press, Oxford (1881).
25. Xue, Q. Z., "Model for thermal conductivity of carbon nanotube-based composites", *Physica B,* 368 (2005) 302-307.
26. Sirelkhatim, A., Mahmud, S., Seeni, A., Kaus, N. H. M., Ann, L. C., Bakhori, S. K. M., Hasan, M. D. "Review on Zinc Oxide Nanoparticles: Antibacterial Activity and Toxicity Mechanism", *Nano-Micro Letters*, 7 (2015) 219–242.
27. Bo/jesen, E. D., So/ndergaard, M., Christensen, M., Iversen, B. B., "Particle size effects on the thermal conductivity of ZnO", *AIP Conference Proceedings*, 1449 (2012) 335.
28. Choudhary, S. Sachdeva, A., Kumar, P., "Influence of stable zinc oxide nanofluid on thermal characteristics of flat plate solar collector. *Renewable Energy*, 152, (2020) 1160-1170.
29. Sheikholeslami, M. "Numerical analysis of solar energy storage within a double pipe utilizing nanoparticles for expedition of melting", *Solar Energy Materials and Solar Cells*, 245 (2022) 111856

30. Mallakpour, S., Dinari, M. and Azadi, E., "Poly (vinylalcohol) Chains Grafted onto the Surface of Copper Oxide Nanoparticles: Application in Synthesis and Characterization of Novel Optically Active and Thermally Stable Nanocomposites Based on Poly (amide-imide) Containing N-trimellitylimido-L-valine Linkage", *International Journal of Polymer Analysis and Characterization*, 20 (2015) 82-97.
31. Ramesh, C., Hariprasad, M., Ragunathan, V., Jayakumar, N. "A novel route for synthesis and characterization of green Cu2O/PVA nanocomposites", *European Journal of Applied Eng. Sci. Res*., 1 (2012) 201–206.
32. Bay, M. A., Khademieslam, H.., Bazyar, B., Najafi, A., Hemmasi, A.H., "Mechanical and Thermal Properties of Nanocomposite Films Made of Polyvinyl Alcohol/Nanofiber Cellulose and Nanosilicon Dioxide using Ultrasonic Method", *International Journal of Nanoscience and Nanotechnology*, 17(2021) 65-76.
33. Zhang, L., Jiang, Y., Ding, Y., Povey, M., York, D., "Investigation into the antibacterial behaviour of suspensions of ZnO nanoparticles (ZnO nanofluids)", *Journal of Nanoparticle Research*, 9 (2007) 479–489.
34. Li, H., Wang, L., He, Y., Hu, Y., Zhu, J. and Jiang, B., "Experimental investigation of thermal conductivity and viscosity of ethylene glycol based ZnO nanofluids", *Applied Thermal Engineering*, 88 (2015) 363-368.
35. Singh, D. K., Pandey, D. K., Yadav, R. R., Singh, D., "A study of nanosized zinc oxide and its nanofluids", *PRAMANA-Journal of Physics*, 78 (2012) 759–766.
36. Sagadevan, S., Shanmugam, S., "A Study of Preparation, Structural, Optical, and Thermal Conductivity Properties of Zinc Oxide Nanofluids", *Journal of Nanomedicine and Nanotechnology*, S6 (2015) 003.
37. Nagvenkar, A. P., Deokar, A., Perelshtein, I., Gedanken, A., "A one-step sonochemical synthesis of stable ZnO-PVA nanocolloid as a potential biocidal agent", *Journal of Materials Chemistry B,* 4 (2016) 2124-2132.
38. Akilu, S., Sharma, K.V., Baheta, A. T., Mamat, R. A., "Review of Thermophysical Properties of Water Based Composite Nanofluids", *Renewable and Sustainable Energy Reviews*, 66 (2016) 654–678.
39. M. Sheikholeslami, M. Jafaryar, M. BarzegarGerdroodbary, Amir H. Alavi, "Influence of novel turbulator on efficiency of solar collector system", *Environmental Technology & Innovation*, (2022) 102383
40. Esfe, M. H., Arani, A. A. A., Badi, R. S., Rejvani, M., "ANN modeling, cost performance and sensitivity analyzing of thermal conductivity of DWCNT–SiO 2/EG hybrid nanofluid for higher heat transfer", *Journal of Thermal Analysis and Calorimetry*, 131 (2018) 2381–93.
41. Yıldız, C., Arıcı, M., Karabay, H. "Comparison of a theoretical and experimental thermal conductivity model on the heat transfer performance of Al_2O_3-SiO_2/water hybrid-nanofluid", *Int International Journal of Heat and Mass Transfer*, 140 (2019) 598-605.
42. Pourrajab, R., Noghrehabadi, A., Hajidavalloo, E., Behbahan, M., "Investigation of thermal conductivity of a new hybrid nanofluids based on mesoporous silica modified with copper nanoparticles: Synthesis, characterization and experimental study", *J. Mol. Liq*., 300 (2020) 112337.
43. Hamilton, R. L., Crosser, O. K, "Thermal conductivity of heterogeneous two-component systems", Industrial *Engineering and Chemistry Fundamentals*, 1 (1962) 187–191.
44. Kumar, R., Kumar, R., Sheikholeslami, M., Chamkha, A. J., "Irreversibility analysis of the three dimensional flow of carbon nanotubes due to nonlinear thermal radiation and quartic chemical reactions", *Journal of Molecular Liquids*, 274 (2019) 379-392.
45. Takabi, B., Salehi, S., "Augmentation of the heat transfer performance of a sinusoidal corrugated enclosure by employing hybrid nanofluids", *Advance in Mechanical Engineering*, (2014) 147059.
46. Subramaniyan, A. and Ilangovan, R., "Thermal Conductivity of Cu_2O-TiO_2 Composite -Nanofluid Based on Maxwell model", *International Journal of Nanoscience and Nanotechnology*, 11 (2015) 59-62
47. Sheikholeslami, M., Jafaryar, M., Gerdroodbary, M. B., Alavi, A. H., "Influence of novel turbulator on efficiency of solar collector system", *Environmental Technology and Innovation*, 26 (2022) 102383.
48. Okonkwo, E. C., Wole‐Osho, I., Almanassra, I. W., Abdullatif, Y. M. and Al‐Ansari, T. An updated review of nanofluids in various heat transfer devices. *J. Therm, Anal. Calor*., 145 (2021) 2817-2872
49. Kakarndee, S., Nanan, S., "SDS capped and PVA capped ZnO nanostructures with high photocatalytic performance toward photo degradation of reactive red (RR141) azo dye", *Journal of Environmetal Chemical Engineering*, 6 (2018) 74–94.
50. Hemalatha, K. S., Rukmani, K., Suriyamurthy, N., Nagabhushana, B. M., "Synthesis, characterization and optical properties of hybrid PVA–ZnO nanocomposite: A composition dependent study", *Materials Research Bulletin*, 51 (2014) 438–446.
51. Suganthi, K. S., Rajan, K. S., "Metal oxide nanofluids: Review of formulation, thermo-physical properties, mechanisms, and heat transfer performance", *Renewable and Sustainable Energy Reviews*, 76 (2017) 226–255.
52. Yua, F., Chena, Y., Liang, X., Xua, J., Lee, C., Liang, Q., Taoa, P., Denga, T., "Dispersion stability of thermal nanofluids", *Progress in Natural Science: Materials International*, 27 (2017) 531–542.
53. Bhagat, U. K., More, P.V., Khanna, P. K., "Study of Zinc Oxide Nanofluids for Heat Transfer Application", *SAJ Nanoscience and Nanotechnology*, (2015) 101.

54. Ghozatloo, A., Niassar, M. S., Rashidi, A., “Effect of Functionalization Process on Thermal Conductivity of Graphene Nanofluids” *International Journal of Nanoscience and Nanotechnology*,13 (2017) 11-18.
55. Jiang, J., Oberdörster, G., Biswas, P., “Characterization of size, surface charge, and agglomeration state of nanoparticle dispersions for toxicological studies”, *Journal of Nanoparticle Research*, (2009) 11 77–89.
56. Almeida, T .C. A., Larentis, A. L., Ferraz, H. C., “Evaluation of the Stability of Concentrated Emulsions for Lemon Beverages Using Sequential Experimental Designs”,*PLOS ONE*, 10 (2015) e0118690.
57. Kouchakzadeh, H., Shojaosadati, S. A., Maghsoudi, A., Farahani, E. V., “Optimization of PEGylation Conditions for BSA Nanoparticles Using Response Surface Methodology”, *AAPS PharmSciTech*, 11 (2010), 1206-1211.
58. Kanti, P. K, Sharma, K. V., Said, Z., Jamei , M., Yashawantha, K. M., “Experimental investigation on thermal conductivity of fly ash nanofluid and fly ash-Cu hybrid nanofluid: prediction and optimization via ANN and MGGP model”, *Particlulate Science and Technology*, 40 (2021) 182-195
59. Kanti, P., Sharma, K. V., Ramachandra, C. G., Azmi, W. H., “Experimental determination of thermo physical properties of Indonesian fly-ash nanofluid for heat transfer applications”, *Particlulate Science and Technology*, 39 (2021) 597-606.